Int. J. Electrochem. Sci., 14 **(2019)** 9098 – 9111, doi: 10.20964/2019.09.77

International Journal of ELECTROCHEMICAL SCIENCE
www.electrochemsci.org

Electrochemical Sensor Platform for 8-Hydroxy-2′-Deoxyguanosine Detection Based on Carboxyl-Functionalized Carbon-Allotropic Nanomaterials Wrapped Gold Nanoparticles Modified Electrode

Zhengjun Yi, Jinjuan Qiao, Ying Wang, Kunshan Gao, Ronglan Zhao and Xiangying Meng**

Department of Laboratory Medicine, Weifang Medical University, Weifang, Shandong 261053, PR China
*E-mail: mengxiangying85730@126.com, ronglanzhao@wfmc.edu.cn

Received: 12 May 2019 / *Accepted:* 14 July 2019 / *Published:* 5 August 2019

As a typical biomarker of oxidative DNA damage, 8-hydroxy-2′-deoxyguanine (8-OHdG) has received considerable attention in recent years, because elevated levels of urinary 8-OHdG are typically associated with various diseases related to oxidative stress. However, the accurate identification and quantification of 8-OHdG in human urine is generally confounded by its trace content and complex matrices. In this work, a facile and effective electrochemical sensor for urinary 8-OHdG detection was constructed based on carboxyl-functionalized carbon-allotropic nanomaterials (GO-COOH/MWCNTs-COOH) wrapped gold nanoparticles (Au NPs), which resulted in modified electrode. The sensing material consisting of GO-COOH, MWCNTs-COOH, polyethyleneimine (PEI), and Au NPs was fabricated by self-assembly of negatively charged Au NPs onto positively charged PEI-wrapped GO-COOH and MWCNTs-COOH through electrostatic interactions. The electrochemical experiments demonstrated that the biosensor showed high electrochemical performance on the oxidation of 8-OHdG and efficiently alleviated the interferences from uric acid (UA) with the help of uricase. According to differential pulse voltammetry (DPV) results, the oxidation peak currents correlated linearly with the concentration of 8-OHdG in the ranges of 0.014 - 0.14 μM (R^2 = 0.9916), 0.14 - 1.41 μM (R^2 = 0.9954), and 1.41 - 14.12 μM (R^2 = 0.9915) with a detection limit (S/N = 3) of 7.06 nM. In addition, the results of analytical detection of 8-OHdG in human urine samples were satisfactory with a very high recovery percentage. Therefore, it is believed that the proposed sensor is a promising candidate for risk assessment of various diseases related to oxidative stress.

Keywords: 8-Hydroxy-2′-deoxyguanine; Electrochemical biosensor; Gold nanoparticles; Carboxyl-functionalized graphene oxide; Carboxyl-functionalized multi-walled carbon nanotubes

1. INTRODUCTION

One of the most common stable products of oxidative DNA damage induced by reactive oxygen species, 8-hydroxy-2′-deoxyguanosine (8-OHdG), has been widely used for the evaluation of in vivo oxidative stress [1]. According to experimental reports, an elevated level of 8-OHdG in body fluids is typically correlated with various diseases, such as cancers [2], ageing [3], diabetes [4], and neurological disorders [5]. It is generally accepted that the level of 8-OHdG excreted in urine is directly related to the extent of the whole-body oxidative DNA damage [6]. Therefore, the level of urinary 8-OHdG has been proposed to be the preferred choice for risk assessment of various diseases related to oxidative stress due to it being easily obtained in a noninvasive manner from the patient. Nevertheless, measuring urinary 8-OHdG is challenging because of its low concentration and the complexity resulting from interfering substances present in urine. The content of 8-OHdG in healthy human urine has been reported to be below 100 nM [7]. Thus, the development of highly sensitive and selective analytical approaches for measuring the urinary levels of 8-OHdG is of great significance for related disease risk evaluation and early diagnosis.

Currently, many different analytical techniques have been reported for 8-OHdG detection, including post ^{32}P-labelling methods [8], an enzyme-linked immunosorbent assay (ELISA) [9], high-performance liquid chromatography with electrochemical detection (HPLC-ECD) [10], capillary electrophoresis with ultraviolet detection (CE-UV) [11], electrochemical detection (CE-ECD) [12], laser-induced fluorescence detection (CE-LIF) [13, 14], high-performance liquid chromatography-mass spectrometry (HPLC-MS) [15], and electrochemiluminescence immunosensor detection [16]. No matter what kinds of techniques have been developed for 8-OHdG detection, the key points usually focus on how to improve the sensitivity and accuracy of the test. However, these analytical approaches mentioned above generally suffer from at least one of the following issues: having tedious clean-up procedures or sample treatment, being time-consuming, having complex and expensive equipment, and/or requiring specially trained operators. Compared to other analytical methods, the electrochemical sensing method offers not only a simple apparatus, easy automation and operation, great potential for miniaturization, a short response time, and low cost but also high sensitivity [17]. Thus, a growing number of electrochemical biosensors for effective quantification of 8-OHdG have been reported in recent years based on the electrochemical oxidation activity of 8-OHdG [4, 17-19]. Overall, the most common efforts that for the sensitivity and accurate quantification of urinary 8-OHdG have been mainly made by modifying of the working electrode using nanomaterials and/or polymers [19, 20], indicating the importance of the support nanomaterial for electrochemical measurement of 8-OHdG.

With the continuous and rapidly increasing advancements made in the field of nanoscience and nanotechnology, various nanomaterials, such as carbon nanomaterials, noble metal nanoparticles, metal oxide nanostructures, semiconductor nanoparticles, and nanocomposites, have been widely employed to fabricate electrochemical biosensors with the aim of accelerating electron transfer and enhancing the electrical signals. Among these nanomaterials, carbon nanomaterials especially graphene oxide (GO) and carbon nanotubes (CNTs) have attracted growing interest in the electrochemistry field due to their unique structures and superior properties, such as relatively large surface area, strong adsorptive ability, high chemical stability and excellent electric conductivity [18,

21, 22]. Nevertheless, the flat shape of GO leads it to undergo π-stacking, where it easily sticks to each other due to the van der Waals interactions, thereby decreasing its surface area to a large extent. On the other hand, CNTs, as another favourable carbon nanomaterial, usually show lower charge density and poor dispersibility in most solvents [6]. To overcome these problems, the hybridization of GO and CNTs was performed by effectively introducing CNTs between GO nanosheets; this material not only displays a high charge density and large surface area but also effectively enhanced conductivity [6, 23-25]. The excellent performance of the GO/CNT hybrid can be attributed to the synergistic effect exhibited by the two different forms of carbon nanomaterial, where the 3D network of CNTs prevents the restacking and agglomeration of GO, and the water solubility and dispersibility of GO leads to the effective and stable dispersion of CNTs [6]. Therefore, GO/CNT hybrids could be promising nanocomposites for the development of surface modified electrochemical sensors. Moreover, considerable efforts have also revealed that combining noble metal nanoparticles with carbon-based nanomaterials can serve as an ideal electrode surface modification for developing electrochemical sensors. Gold nanoparticles (Au NPs) are the most extensively used metal nanoparticles for electrode surface modification due to their unique properties such as their high surface-to-volume ratio, high biocompatibility and good conductivity. Although there are several papers on the use of Au NP-decorated carbon-based supports for various purposes, the integration of Au NPs with carboxyl-functionalized GO (GO-COOH) and carboxyl-functionalized MWCNT (MWCNT-COOH) hybrid networks for 8-OHdG detection has not been reported. Specifically, GO-COOH and MWCNTs-COOH with an increased oxygen content can significantly increase their solubility and dispersion in solvents, which might greatly enhance their further application in electrochemical sensing of 8-OHdG.

From all these findings, we were encouraged to develop a facile electrochemical sensor for the determination of 8-OHdG. The fabrication process of the proposed electrochemical sensor is illustrated in Scheme 1. In this work, a sensing material consisting of GO-COOH, MWCNTs-COOH, polyethyleneimine (PEI) and Au NPs was fabricated by self-assembly of negatively charged Au NPs onto positively charged PEI-wrapped GO-COOH and MWCNTs-COOH through electrostatic interactions. The GO-COOH/MWCNT-COOH/PEI/Au NP hybrid modified electrode was prepared by drop-coating a GO-COOH/MWCNT-COOH/PEI/Au NP dispersion on the surface of a bare glassy carbon electrode (GCE). The synergistic behaviour of the two carboxyl-functionalized allotropic forms of carbon and Au NPs showed excellent electrocatalytic activity towards the oxidation of 8-OHdG with many advantages, such as high sensitivity, stability and reproducibility. The potential application of the modified electrode for the quantification of 8-OHdG in human urine samples was also investigated. The presence of large quantities of uric acid (UA) severely affected the sensitive detection of 8-OHdG. Uricase has been employed to successfully eliminate the interferences of the large amounts of UA, which makes it possible for the trace detection of 8-OHdG in urine samples.

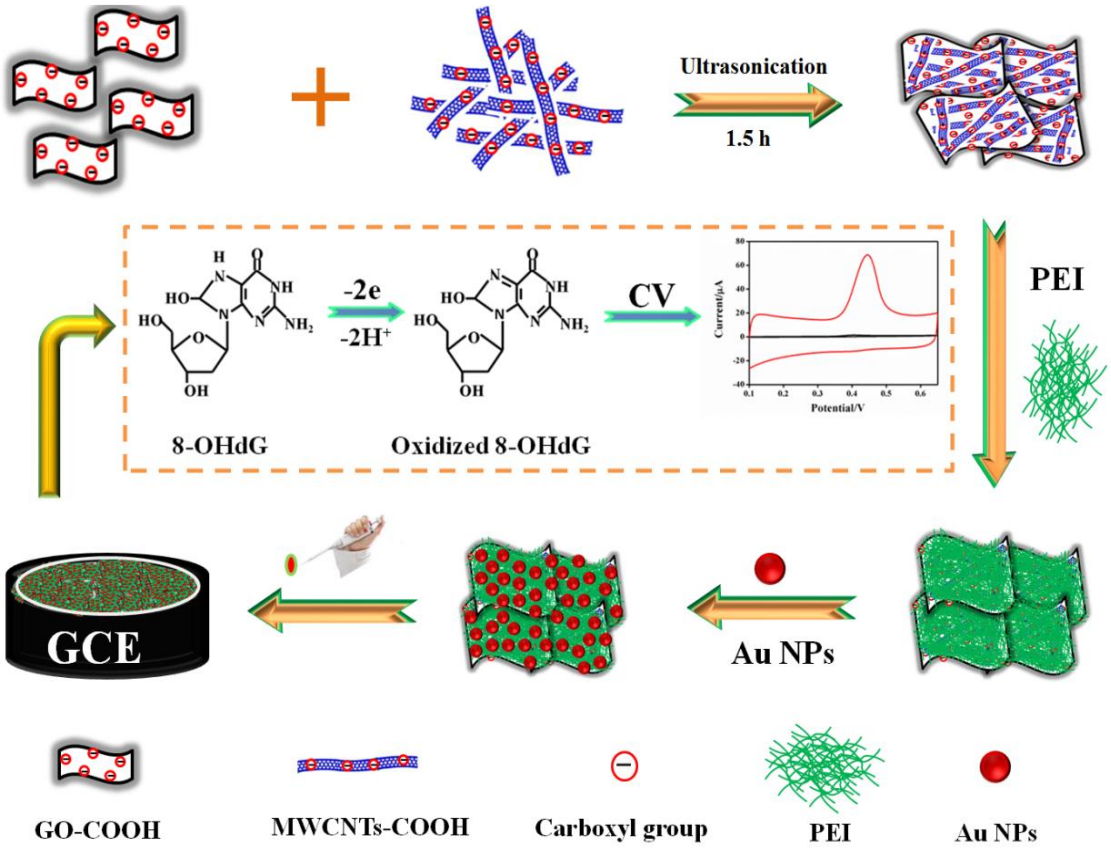

Scheme 1. Illustration of the preparation process of the proposed electrochemical sensor platform.

2. EXPERIMENTAL

2.1. Materials and instruments

8-OHdG, uric acid (UA), gold chloride trihydrate ($HAuCl_4 \cdot 3H_2O$) were purchased from Sigma Aldrich, China. Uricase (≥ 20 u/mg) was purchased from Shanghai Macklin Biochemical Co., Ltd. (Shanghai, China). GO-COOH and MWCNTs-COOH were obtained from Hangzhou Hangdan Photoelectric Technology Co. Ltd. PEI and sodium citrate dehydrate was obtained from Aladdin reagent Co., Ltd. (Shanghai, China). Sodium dihydrogen phosphate ($NaH_2PO_4 \cdot 2H_2O$), disodium hydrogen phosphate ($Na_2HPO_4 \cdot 12H_2O$), sodium chloride (NaCl), potassium chloride (KCl) were purchased from Sinopharm Chemical Reagent Co., Ltd. (Shanghai, China). All of the chemicals used in this work were of analytical grade and used without further purification. All aqueous solutions were prepared with deionized water.

Transmission electron microscopy (TEM) images and energy dispersive X-ray spectroscopy (EDS) elemental analysis were all conducted on a JEM-2100 TEM instrument (JEOL, Japan). All electrochemical measurements were carried out on a CHI660E electrochemical workstation (Chenhua Instrument Company of Shanghai, China) with a conventional three-electrodes system composed of a platinum auxiliary, an Ag/AgCl (saturated KCl) reference, and a glassy carbon working electrode with a diameter of 3 mm. All tests were conducted in a phosphate buffer solution at room temperature.

2.2. Preparation of Au NPs

Au NPs with average diameter 13 nm were synthesized by reduction of the $HAuCl_4$ solution with sodium citrate according to the procedures reported previously [26]. In a typical procedure, all glassware used in the following procedures were soaked overnight in a bath of freshly prepared aqua regia (HCl/HNO_3, 3:1, v/v), rinsed thoroughly with a large amount of deionized water, and oven dried at 60 °C prior to use. After that, 96 mL of deionized water and 4 mL of $HAuCl_4$ (1 wt%) were added to a conical flask with vigorous stirring followed by the rapid addition of 2 mL of trisodium citrate (5 wt%). When the mixture turned into wine red, the solution was kept boiling for 5 another minutes. Subsequently, the heating source was removed. After cooling to room temperature under conditions of agitation, the resulting solution of Au NPs with negative charge was put into a brown bottle and stored at 4 °C for further use.

2.3. Preparation of GO-COOH /MWCNT-COOH/PEI/Au NP nanocomposites

The GO-COOH/MWCNT-COOH/PEI/Au NP hybrid nanocomposites were directly prepared by the simple electrostatic adsorption. Briefly, 10 mg of carboxyl functionalized graphene oxide (GO-COOH) and 10 mg of carboxyl functionalized single-walled carbon nanotubes (MWCNTs–COOH) in a mass ratio of 1:1 were added together into 50 mL of 1.0 M NaCl solution to form a homogeneous solution under ultrasonication for 1.5 h. After that, 80 mg of PEI was added and continuously sonicated for another 2.5 h. Then, the resulting solution was centrifuged at 5000 rpm for 10 min and washed with deionized water to remove excess PEI and NaCl. Next, the product was resuspended in 10 mL of the as-prepared Au NPs solution and allowed to react in the refrigerator overnight at 4°C. Afterwards, the product were collected by centrifugation and further washed with deionized water. Finally, the product was resuspended in 5 mL deionized water. And the as-prepared GO-COOH/MWCNT-COOH/PEI/Au NP nanocomposites homogeneous suspension solution was obtained by the intermediate medium of PEI.

2.4. Fabrication of the modified electrodes

Prior to modification, the bare GCE was polished successively with 0.3 and 0.05 μm alumina slurry on a fine chamois. After that, the electrode was successively ultrasonically washed in nitric acid (1:1), ethanol, and deionized water for 3 min, respectively. After dried in air at room temperature, 5.0 μL of the as-prepared GO/MWCNT/PEI/Au NP solution (1.0 mg/mL) was dripped onto the working area of the pretreated GCE and dried in air at room temperature. After being washed with deionized water, the resulted electrode denoted as GCE/GO-COOH/MWCNT-COOH/PEI/Au NP was ready for further use. For electrode comparison, four different electrodes were also prepared with or without GO-COOH, MWCNTs-COOH, PEI, and Au NPs, respectively.

3. RESULTS AND DISCUSSION

3.1. Characterization of the obtained GO-COOH/MWCNT-COOH/PEI/Au NP nanocomposites

The morphologies of the as-prepared GO-COOH, MWCNTs-COOH, GO-COOH/MWCNTs-COOH, Au NPs and GO-COOH/MWCNT-COOH/PEI/Au NP hybrid nanocomposites were characterized by TEM. As shown in Figure 1A, the TEM image of pure GO-COOH shows a typically smooth and planar sheet with a partially wrinkled microstructure. Figure 1B shows that pure MWCNTs-COOH are naturally entangled and disordered. Figure 1C shows that the GO-COOH/MWCNT-COOH hybrids are well assembled with MWCNTs-COOH hooked onto GO-COOH nanosheets, which could be attributed to the π–π stacking interaction between the sidewalls of MWCNTs-COOH and hydrophobic regions of GO-COOH [23]. After the addition of negatively charged Au NPs (Figure 1D), a typical image of the GO-COOH/MWCNT-COOH/PEI/Au NP hybrid nanocomposites indicates that Au NPs are distributed on the whole surface of the GO-COOH/MWCNTs-COOH by the intermediate medium of PEI which endows many positively charged active sites (Figure 1E). The particle size of Au NPs on GO-COOH/MWCNTs-COOH was estimated to be approximately 13 nm. In addition, the formation of the GO-COOH/MWCNT-COOH/PEI/Au NP hybrid was further confirmed by EDS. From Figure 1F, the presence of the peaks corresponding to the C, O, and Au elements confirmed the formation of Au NPs attached to the GO-COOH/MWCNT-COOH nanostructure.

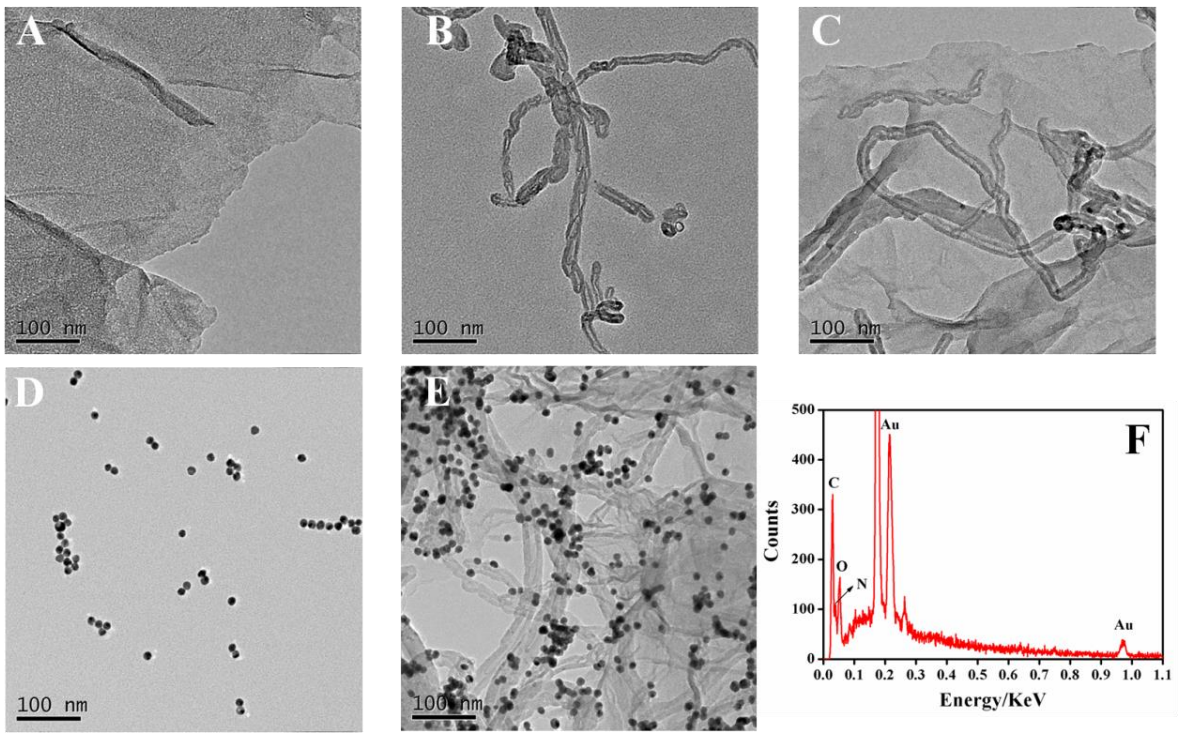

Figure 1. TEM images of (A) GO-COOH, (B) MWCNT-COOH, (C) GO-COOH/MWCNT-COOH, (D) Au NPs, and (E) GO-COOH/MWCNT-COOH/PEI/Au NP hybrid; (F) EDS of the GO-COOH/MWCNT-COOH/PEI/Au NP hybrid.

3.2. Electrochemical behaviours of 8-OHdG on GCE/GO-COOH/MWCNTs-COOH/PEI/Au NPs

The response of the electrochemical oxidation of 8-OHdG to different modified electrodes was examined by the CV method in a potential range from 0.1 to 0.65 V. Figure 2 shows the CV of differently modified GCEs taken at a scan rate of 50 mV/s in 0.1 M pH 7.0 phosphate buffer solution (PBS) containing 7.06 μM 8-OHdG using a bare GCE (curve a) and GO-COOH (curve b), MWCNT-COOH (curve c), GO-COOH/MWCNT-COOH (curve d), GO-COOH/MWCNT-COOH/PEI (curve e) and GO-COOH/MWCNT-COOH/PEI/Au NP (curve f) modified GCEs. Figure 2 shows that the bare GCE displayed a weak irreversible oxidation peak. The electrochemical signals were enhanced when GO-COOH and MWCNTs-COOH and the GO-COOH/MWCNT-COOH and GO-COOH/MWCNT-COOH/PEI nanocomposites were dropped on the surface of GCE, indicating the excellent electrochemical performance of the carboxyl-functionalized carbon-allotropic nanomaterials on the oxidation of 8-OHdG. It is worth noting that the peak current of 8-OHdG at GCE/GO-COOH/MWCNTs-COOH/PEI decreased in comparison with that at GCE/GO-COOH/MWCNTs-COOH. The possible reason is that the active amino groups present in PEI at high density can be protonated at pH < 8 [27] and highly protonated PEI is not conducive to the adsorption of 8-OHdG on the electrode surface because 8-OHdG, with a pKa1 of 8.6, mainly exists as a positively charged form in solutions at pH < 8.6 [28, 29]. After the introduction of Au NPs, the GO-COOH/MWCNT-COOH/PEI/Au NP electrode gave rise to the largest oxidation peak current, which was approximately 56.5 times higher than that with the bare electrode. This difference was because the synergistic effect between GO-COOH, MWCNTs-COOH and Au NPs increased the effective surface area and improved the electron exchange kinetics between the nanocomposites and the 8-OHdG. These results indicated that the GO-COOH/MWCNT-COOH/PEI/Au NP nanocomposite made great contributions to the improvement of the sensitivity of the GCE sensor.

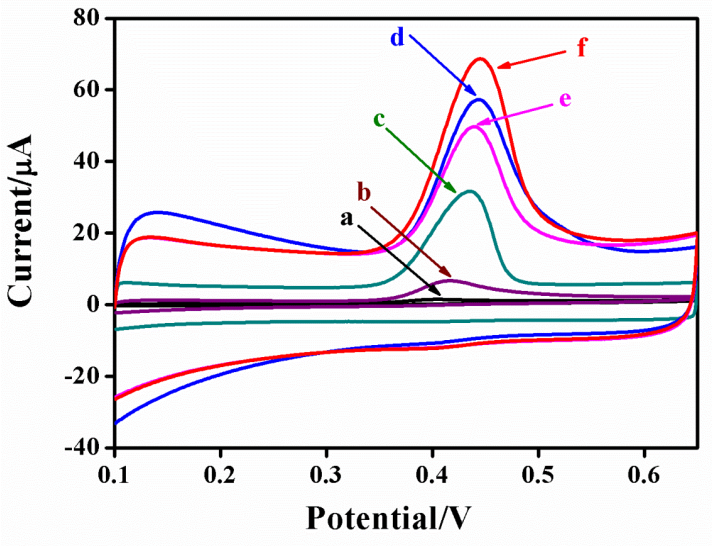

Figure 2. Cyclic voltammograms of bare (a), GO-COOH (b), MWCNT-COOH (c), GO-COOH/MWCNT-COOH (d), GO-COOH/MWCNT-COOH/PEI (e) and GO-COOH/MWCNT-COOH/PEI/Au NP (f) modified GCEs at the scan rate of 100 mV/s in 0.1 M pH 7.0 PBS containing 7.06 μM 8-OHdG.

3.3. Effect of scan rate and pH value

To investigate the reaction kinetics, CV measurements were performed in 0.1 M PBS (pH 7) containing 7.06 μM 8-OHdG on GCE/GO-COOH/MWCNTs-COOH/PEI/Au NPs at varying scan rates from 5 to 350 mV/s. As shown in Figure 3A, a well-defined oxidation peak was observed at + 0.404 V that gradually shifted towards positive values as the scan rate increased. Meanwhile, the peak currents linearly increased as the scan rate increased. The linear regression equation for this behaviour is I_p (μA) = 0.9166 v (mV/s) + 11.93 (R^2 = 0.9920), indicating that the oxidation of 8-OHdG on GCE/GO-COOH/MWCNTs-COOH/PEI/Au NPs is an adsorption-controlled electrode process which is in good agreement with other researchers [4, 7].

It is well known that the pH of the supporting electrolyte significantly affects the peak parameters, moreover, it also provides insight into the number of involved protons and electrons [6]. Therefore, the influence of pH on the electrochemical behaviour of 8-OHdG was further investigated in the range of 6.0 - 12.0. As shown in Figure 3B, the oxidation peak potential of 8-OHdG was found to shift negatively with increasing pH, indicating that protons participate in the oxidation of 8-OHdG. The linear dependence of the peak potential (Ep) on pH can be expressed by the following equation: E_p = 0.8609 - 0.0595 pH (R^2 = 0.9994). The slope of - 0.0595 V pH^{-1} value is close to the theoretical Nernstian value of - 0.059 V pH^{-1}, suggesting that the numbers of protons and electrons involved were equal in the oxidation of 8-OHdG. The result is in accordance with results reported previously [6, 18].

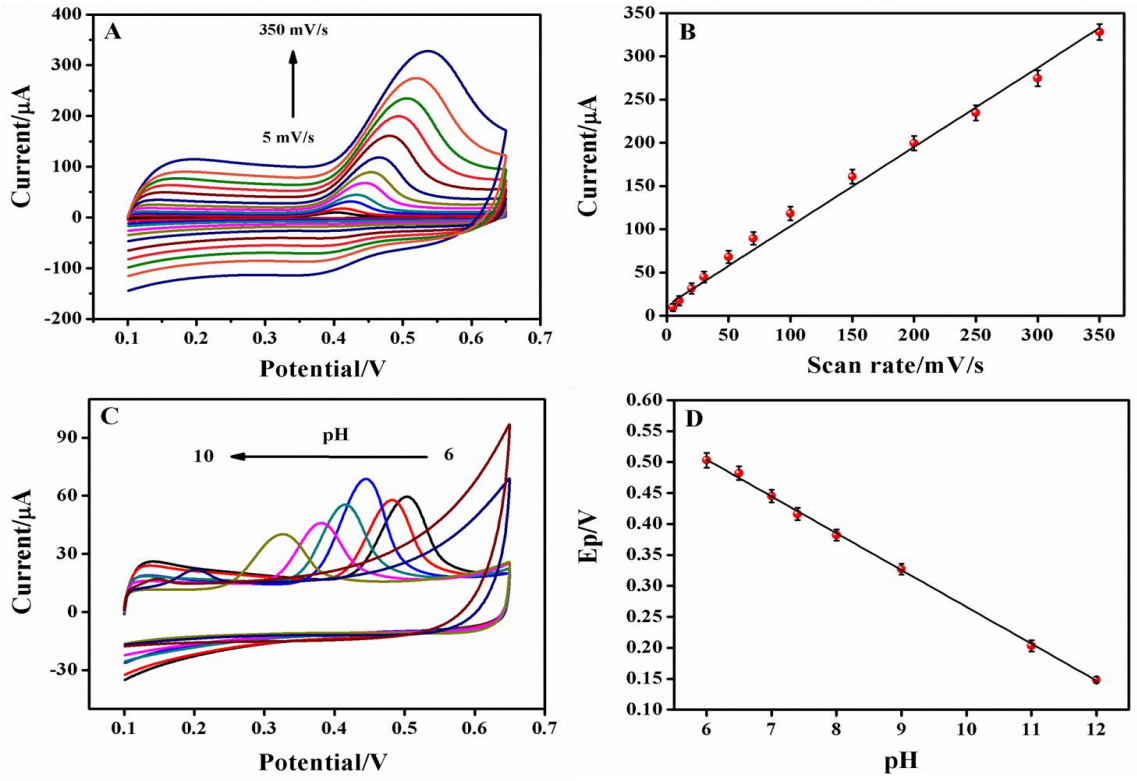

Figure 3. (A) CVs of GCE/GO-COOH/MWCNTs-COOH/PEI/Au NPs at different scan rates (5 - 350 mV/s) in 0.1 M PBS (pH 7.0) containing 7.06 μM 8-OHdG. (B) the plot of Ip (μA) vs. v (mV/s). (C) CVs of 7.06 μM 8-OHdG on GCE/GO-COOH/MWCNTs-COOH/PEI/Au NPs in different pHs: 6.0, 6.5, 7.0, 7.4, 8, 9, 11, 12. (D) the plot of Ep (V) vs. pH.

3.4. Effect of preconcentration time

For an adsorption-controlled electrode process, analyte preconcentration is a simple and efficient way to improve the detection sensitivity. Therefore, the effect of preconcentration time on the oxidation current of 8-OHdG was carefully studied. Considering that stirring of the tested solution might affect the efficiency of preconcentration, this effect was first examined. Figure 4A displays the CV of 8-OHdG at GCE/GO-COOH/MWCNTs-COOH/PEI/Au NPs after a preconcentration time of 5 min without stirring (curve (a)) and with constant stirring (curve (b)). The oxidation peak current of 8-OHdG with moderate stirring is approximately 2.57 times higher than that without stirring, indicating that stirring can effectively improve the efficiency of preconcentration. Therefore, the effect of preconcentration time on the oxidation peak current of 8-OHdG was investigated under constant stirring using a magnetic stirrer. As seen in Figure 4B, the results show that the peak current increased rapidly when the accumulation time varied from 1 min to 5 min and then increased relatively slowly once the preconcentration time was longer than 5 min. This phenomenon can be attributed to the fact that the amount of 8-OHdG to be concentrated in the GO-COOH/MWCNT-COOH/PEI/Au NP film reaches a relative saturation state for adsorption on the working electrode surface. In addition, it should be noted that the greatly increased oxidation signals of 8-OHdG on the GCE/GO-COOH/MWCNTs-COOH/PEI/Au NPs reveal the improved accumulation ability of GO-COOH/MWCNT-COOH/PEI/Au NP nanocomposites towards 8-OHdG, which can be explained by two aspects. On the one hand, GO-COOH, MWCNTs-COOH and Au NPs have larger surface areas and more accumulation sites than bare electrodes. On the other hand, 8-OHdG (pK_{a1} = 8.6 and pK_{a2} = 11.7) exists in cationic form in the solutions at pH < 8.6 [28, 29], and it is more easily adsorbed onto the surface of the negatively charged GO-COOH/MWCNT-COOH/PEI/Au NP hybrid modified GCE in pH 7.0 PBS than onto the surfaces of the other electrodes. Therefore, the prepared GCE/GO-COOH/MWCNTs-COOH/PEI/Au NPs greatly improved the preconcentration efficiency for 8-OHdG, which results in the high detection sensitivity of the developed method. Finally, the preconcentration time of 5 min was selected as the best compromise between the detection sensitivity and the time required for the analysis.

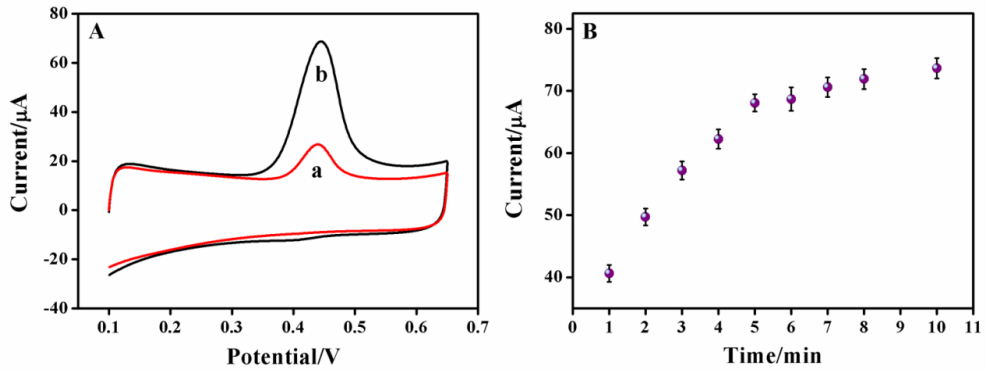

Figure 4. (A) CVs on GCE/GO-COOH/MWCNTs-COOH/PEI/Au NPs under different accumulation conditions for 5 min. (a) Without stirring. (b) With stirring. (B) Dependence of the peak current on the accumulation time at GCE/GO-COOH/MWCNTs-COOH/PEI/Au NPs. CV measurements were performed in 0.1 M pH 7.0 PBS solution containing 7.06 μM 8-OHdG at a scan rate of 50 mV/s.

3.5. Analytical performance of the 8-OHdG sensor

The electrochemical determination of 8-OHdG was investigated by differential pulse voltammograms (DPVs). Figure 5A shows that the oxidation peak currents increased with increasing 8-OHdG concentration.

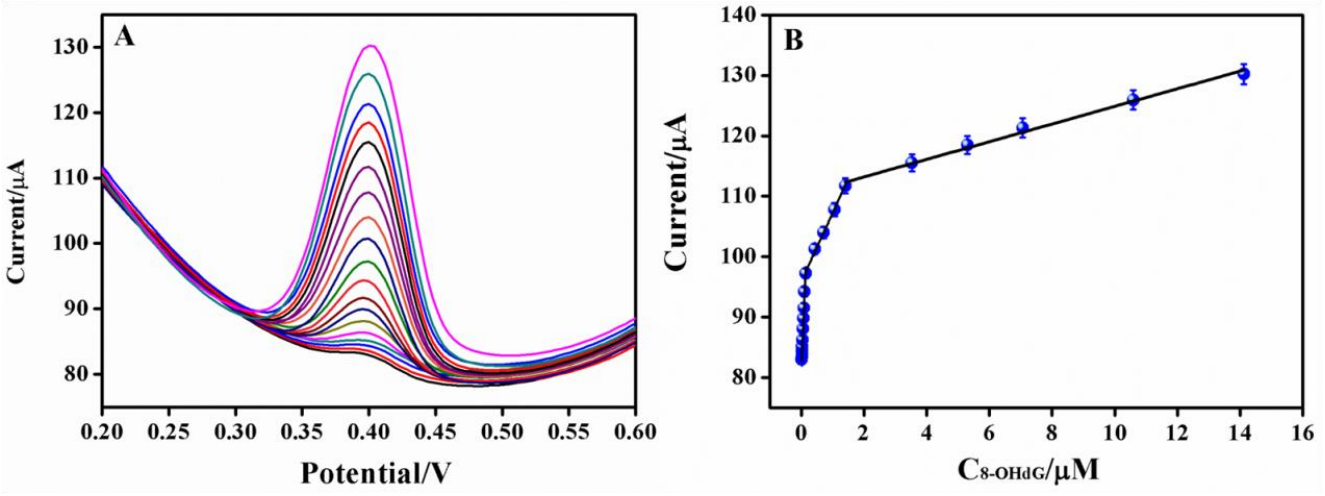

Figure 5. (A) DPVs of different concentration of 8-OHdG on GCE/GO-COOH/MWCNTs-COOH/PEI/Au NPs in 0.1 M pH 7.0 PBS solution at scan rate of 50 mV/s with a wide range of concentrations from 0.014 μM to 14.12 μM. (B) The corresponding calibration curve of the concentration of 8-OHdG.

Table 1. Comparison of different electrochemical sensors for determination of 8-OHdG.

Electrode Materials	Linear range (μM)	LOD (nM)	References
GCE/SWCNTs-Nafon	0.03 - 1.25	8.0	[19]
GCE/CNT-PEI	0.5 - 30	100	[30]
GCE/MWCNT/ErGO	3 - 75	35	[6]
GCE/SWCNT-Lys	0.30 - 10.0	97	[31]
DNA/P3MT/GCE	0.28 - 19.6	56	[32]
GCE/MWCNT	0.056–16	18.8	[33]
GCE/GO-COOH/MWCNTs-COOH/PEI/Au NPs	0.014 - 0.14 0.14 - 1.41 1.41 - 14.12	7.06	This work

Figure 5B shows the corresponding dependence of the oxidation currents on the concentration of 8-OHdG. Linear response ranges were obtained in the range of 0.014 - 0.14 μM, 0.14 - 1.41 μM and 1.41 - 14.12 μM. The regression equations are expressed as follows: I_p (μA) = 121.47 C (μM) - 81.09 (R^2 = 0.9916), I_p (μA) = 11.31C (μM) - 95.94 (R^2 = 0.9954) and Ip (μA) = 1.462C (μM) + 110.3 (R^2 = 0.9915). The limit of detection (LOD) was 7.09 nM (S/N = 3), which might be attributed to the excellent signal amplification with the GO-COOH/MWCNT-COOH/PEI/Au NP hybrid. Moreover, the detection performance of this study was compared with that of several modified electrodes previously reported, and it is presented in Table 1. From Table 1, we can see that the developed sensing platform has a reasonable linear range and either a lower or comparable detection limit for 8-OHdG. The above results indicate that the developed method possesses great potential for reliable determination of 8-OHdG.

3.6. Selectivity, stability and reproducibility of the biosensor

According to the reference results [27], UA, with a similar structure and electrochemical response to 8-OHdG, is considered to be the major interferent for the detection of 8-OHdG because of the relatively high concentrations of UA in real urine samples. To examine the selectivity of the proposed method, the interference of UA in the determination of 8-OHdG was investigated. Figure 6A displays the CV of 0.353 μM 8-OHdG at GCE/GO-COOH/MWCNTs-COOH/PEI/Au NPs in the presence of 100 μM UA (35.3-fold higher concentration of 8-OHdG). Two clear and well-separated oxidation peaks appeared at 0.432 V and 0.365 V, corresponding to the oxidation peaks of 8-OHdG and UA, respectively. The peak of 8-OHdG did not exhibit significant deviation in the presence of a high concentration of interfering UA. The high selectivity of the developed method might be attributed to the electrostatic repulsion between UA anions and the negatively charged GO-COOH/MWCNT-COOH/PEI/Au NP film resulting in the weak adsorption of UA (pKa = 5.7) because it exists in an anionic form in pH 7.0 PBS [27]. Although the GCE/GO-COOH/MWCNTs-COOH/PEI/Au NPs can effectively reduce the interference of UA, the presence of large quantities of UA (above 0.5 mM) still interfered with the trace (below 100 nM) detection of 8-OHdG in a real urine sample, which was commonly chosen as the analysis sample to monitor the level of 8-OHdG in the human body. Thus, it is necessary to reduce or eliminate the interference of UA to fulfill the trace determination of 8-OHdG in urine samples. UA can be oxidized by uricase to allantoin, which is not electrochemically active, indicating that the addition of uricase to the detection solution will remove the interference of UA with the determination of 8-OHdG by the GCE/GO-COOH/MWCNTs-COOH/PEI/Au NPs. As shown in Figure 6B, the peak currents of UA decrease gradually when uricase is successively added into a mixture solution containing 0.353 μM 8-OHdG and 1 mM UA. The UA peak almost disappeared when the concentration of uricase was 50 μg/mL (Figure 6d), indicating that UA had been completely oxidized with uricase as a catalyst. The results demonstrate that the introduction of uricase could effectively eliminate the interference of UA, thus improving the selectivity for the detection of 8-OHdG.

The reproducibility and stability of the modified electrode were the major concerns for practical application. The reproducibility for five modified electrodes was estimated by comparing the oxidation peak currents of 0.353 μM 8-OHdG. The relative standard deviation (RSD) was calculated to be 4.61%, suggesting excellent reproducibility. The operational stability was investigated by utilizing one modified electrode in continuous cyclic potential scans for the detection of 0.353 μM 8-OHdG. The RSD of the oxidation peak currents was 0.54%. Furthermore, the storage stability was also studied. After careful investigation, the oxidation peak currents still retained more than 90% of the current response after storage at 4 °C for one week, indicating the good stability of the fabricated electrode. Hence, it can be concluded that the developed method bears appreciable reproducibility and stability.

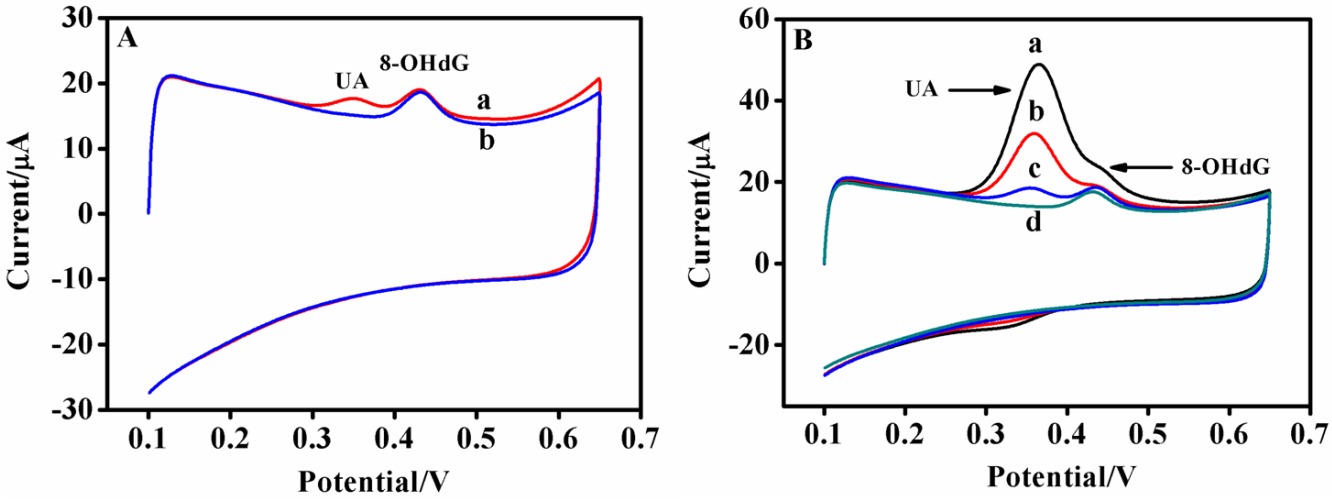

Figure 6. (A) CVs of GCE/GO-COOH/MWCNTs-COOH/PEI/Au NPs in 0.1 M pH 7.0 PBS containing (a) 0.353 μM 8-OHdG + 100 μM UA; (b) 0.353 μM 8-OHdG; (B) CVs of GCE/GO-COOH/MWCNTs-COOH/PEI/Au NPs in 0.1 M pH 7.0 PBS containing (a) 0.353 μM 8-OHdG + 1mM UA; (b) 0.353 μM 8-OHdG + 1 mM UA + 20 μg/mL uricase; (c) 0.353 μM 8-OHdG + 1 mM UA + 40 μg/mL uricase; (d) 0.353 μM 8-OHdG + 1mM UA + 50 μg/mL uricase.

3.7. Real sample analysis

The feasibility and application potential of the proposed method was evaluated by detecting the spiked recovery of 8-OHdG in healthy human urine. Human urine samples from healthy volunteers were first centrifuged at 12,000 rpm for 10 min to remove precipitation. Then, the supernatants were collected and diluted 10 times using 0.1 M PBS (pH 7.0) for the electrochemical determination. After the prepared urine samples were further treated with uricase (60 μg/mL), the obtained spiked recovery results ranged from 99.43% to 101.1% (Table 2), revealing the possibility of using the proposed method for real samples.

Table 2. Recovery results of 8-OHdG at different concentrations spiked into human urine samples.

Sample	Added (μM)	Found (μM)	Recovery (%)
1	0.035	0.0354 ± 0.02	101.1
2	0.14	0.141 ± 0.03	100.7
3	1.06	1.054± 0.03	99.43
4	7.06	7.047± 0.05	99.81

4. CONCLUSIONS

In this work, we successfully prepared a GO-COOH/MWCNT-COOH/PEI/Au NP nanocomposite-modified electrode by drop-casting a GO-COOH/MWCNT-COOH/PEI/Au NP dispersion on the surface of a GCE for 8-OHdG detection. The electrochemical performance of the proposed electrode was investigated carefully, and the electrode showed excellent electrocatalytic activity towards 8-OHdG with high sensitivity, stability and reproducibility; a wide linear range and a low detection limit. Importantly, the as-prepared nanocomposite-modified electrode successfully avoided the interference from UA when uricase was employed, which makes the determination of 8-OHdG in urine samples a potential application for this electrode. In summary, the GO-COOH/MWCNT-COOH/PEI/Au NP nanocomposite is a promising electrode material for constructing a good alternative electrochemical detection system for the effective determination of 8-OHdG, which might offer a possible way to evaluate various diseases related to oxidative stress in biological systems.

ACKNOWLEDGMENTS
We greatly appreciate the support of the Natural Science Foundation of Shandong Province, China (Grant Nos. ZR2016BL19, ZR2017LH057, ZR2018ZC1054 and ZR2017LH055), and the National Natural Science Foundation of China (Grant No. 81770915).

References

1. H.Q. Guo, K.P. Xue, and L.S. Yan, *Sens. Actuators B Chem.*, 171 (2012) 1038.
2. L. Wu, C. Chiou, P. Chang, and J. Wu, *Clin. Chim. Acta*, 339 (2004) 1.
3. K. Tamae, K. Kawai, S. Yamasaki, K. Kawanami, M. Ikeda, K. Takahashi, T. Miyamoto, N. Kato, and H. Kasai, *Cancer Sci.*, 100 (2009) 715.
4. M.Z.H. Khan, X.Q. Liu, Y.F. Tang, and X.H. Liu, *Biosens. Bioelectron.*, 117 (2018) 508.
5. C.M. Chen, J.L. Liu, Y.R. Wu, Y.C. Chen, H.S. Cheng, M.L. Cheng, and D.T.Y. Chiu, *Neurobiol. Dis.*, 33 (2009) 429.
6. Rosy, and R.N. Goyal, *Talanta*, 161 (2016) 735.
7. L.P. Jia, J.F. Liu, and H.S. Wang, *Biosens. Bioelectron.*, 67 (2015) 139.

8. R.C. Gupta, and J.M. Arif, *Chem. Res. Toxicol.*, 14 (2001) 951.
9. P. Rossner, V. Mistry, R. Singh, R.J. Sram, and M.S. Cooke, *Biochem. Biophys. Res. Commun.*, 440 (2013) 725.
10. D. Kato, M. Komoriya, K. Nakamoto, R. Kurita, S. Hirono, and O. Niwa, *Anal. Sci.*, 27 (2011) 703.
11. P.P. Zhang, K.Q. Lian, X.L. Wu, M. Yao, X. Lu, W.J. Kang, and L.L. Jiang, *J. Chromatogr. A*, 1336 (2014) 112.
12. S.W. Zhang, X. Song, W.Y. Zhang, N. Luo, and L.S. Cai, *Sci. Total Environ.*, 450 (2013) 266.
13. X.Y. Meng, X.M. Suo, W.J. Ding, X.J. Li, and Y.S. Ding, *Electrophoresis*, 35 (2014) 1873.
14. X.Y. Meng, Q.R. Liu, and Y.S. Ding, *Electrophoresis*, 38 (2017) 494.
15. D. Chen, and H. Xu, *Mikrochim. Acta*, 186 (2019).
16. T.T. Zhang, H.M. Zhao, X.F. Fan, S. Chen, and X. Quan, *Talanta*, 131 (2015) 379.
17. F. Shahzad, S.A. Zaidi, and C.M. Koo, *Sens. Actuators B Chem.*, 241 (2017) 716.
18. T.Y. Shang, P.L. Wang, X.H. Liu, X.C. Jiang, Z.G. Hu, and X.Q. Lu, *J. Electroanal. Chem.*, 808 (2018) 28.
19. L.F. Yang, B. Wang, H.L. Qi, Q. Gao, C.Z. Li, and C.X. Zhang, *J. Sens.*, (2015).
20. A. Gutierrez, S. Gutierrez, G. Garcia, L. Galicia, and G.A. Rivas, *Electroanalysis*, 23 (2011) 1221.
21. M. Tominaga, N. Watanabe, and Y. Yatsugi, *J. Electroanal. Chem.*, 800 (2017) 156.
22. M. Rizwan, S. Elma, S.A. Lim, and M.U. Ahmed, *Biosens. Bioelectron.*, 107 (2018) 211.
23. S. Cheemalapati, S. Palanisamy, V. Mani, and S.M. Chen, *Talanta*, 117 (2013) 297.
24. B. Rezaei, H.R. Jamei, and A.A. Ensafi, *Biosens. Bioelectron.*, 115 (2018) 37.
25. C.Y. Min, Q.Q. Zhang, C. Shen, D.D. Liu, X.J. Shen, H.J. Song, S.J. Li, D. Xu, X.Y. Lin, and K. Zhang, *RSC Adv.*, 7 (2017) 32574.
26. Y.Q. He, X.B. Zhang, S.Q. Zhang, M.K.L. Kris, F.C. Man, A.N. Kawde, and G.D. Liu, *Biosens. Bioelectron.*, 34 (2012) 37.
27. N.R. Jalal, T. Madrakian, A. Afkhami, and M. Ghamsari, *J. Electroanal. Chem.*, 833 (2019) 281.
28. L.P. Jia, and H.S. Wang, *J. Electroanal. Chem.*, 705 (2013) 37.
29. J.X. Hao, K.B. Wu, C.D. Wan, and Y. Tang, *Talanta*, 185 (2018) 550.
30. A. Gutierrez, S. Osegueda, S. Gutierrez-Granados, A. Alatorre, M.G. Garcia, and L.A. Godinez, *Electroanalysis*, 20 (2008) 2294.
31. A. Gutierrez, F.A. Gutierrez, M. Eguilaz, J.M. Gonzalez-Dominguez, J. Hernandez-Ferrer, A. Anson-Casaos, M.T. Martinez, and G.A. Rivas, *RSC Adv.*, 6 (2016) 13469.
32. Y.H. Wang, J. Li, Y. Liu, R.N. Ma, W.L. Jia, H. Cui, and H.S. Wang, *Sci. China B Chem.*, 52 (2009) 2006.
33. Z.P. Guo, X.H. Liu, Y.L. Liu, G.F. Wu, and X.Q. Lu, *Biosens. Bioelectron.*, 86 (2016) 671.